Chemistry Europe
European Chemical Societies Publishing

WILEY VCH

Excellence in Chemistry Research

Announcing our new flagship journal

- Gold Open Access
- Publishing charges waived
- Preprints welcome
- Edited by active scientists

Meet the Editors of *ChemistryEurope*

Luisa De Cola
Università degli Studi di Milano Statale, Italy

Ive Hermans
University of Wisconsin-Madison, USA

Ken Tanaka
Tokyo Institute of Technology, Japan

ChemPlusChem

Research Article
doi.org/10.1002/cplu.202300017

Chemistry Europe
European Chemical Societies Publishing

www.chempluschem.org

Microwave-Assisted Reductive Amination of Aldehydes and Ketones Over Rhodium-Based Heterogeneous Catalysts

Fabio Bucciol,[a] Emanuela Calcio Gaudino,*[a] Alberto Villa,[b] Maria Carmen Valsania,[c] Giancarlo Cravotto,[a] and Maela Manzoli*[a]

Microwave (MW)-assisted reductive aminations of aldehydes and ketones were carried out in the presence of commercial and homemade heterogeneous Rh-based catalysts. Ultrasound (US) was used to improve dispersion and stability of metal nanoparticles, while commercial activated carbon and carbon nanofibers were used as supports. Moreover, various bio-derived molecules were selected as substrates, and aqueous ammonia was used as a cheap and non-toxic reagent. MW combined with heterogeneous Rh catalysts gave a 98.2% yield in benzylamine at 80 °C with 10 bar H_2 for 1 h; and a 43.3% yield in phenylethylamine at 80 °C and 5 bar H_2 for 2 h. Carbon nanofibers proved to be a better support for the metal active phase than simple activated carbon, since a limited yield in benzylamine (10.6%) but a high selectivity for the reductive amination of ketones was obtained. Thus, raspberry ketone was converted to raspberry amine in a 63.0% yield.

Introduction

Amines are essential bioactive compounds in nature, but also the synthesis of industrial products such as pharmaceuticals[1–4] and polymers.[5–8] Amines are also important as reagents in organic chemistry.[9–11] The reductive amination of aldehydes is a pivotal method in organic synthesis[12] because of the mild reaction conditions, the high atom economy and the abundance of available substrates[13] such as ketones[14,15] though less reactive. Reductive amination can be performed with alkyl amines to obtain secondary or tertiary derivatives, but ammonia is an attractive alternative[16–18] since, albeit less prone to react, it leads to primary amines that can be further modified as required. Ammonia is a cheap reagent, but its handling poses some challenges compared to common organic reagents because it is usually handled only as a gas or in aqueous solutions. Metal-based catalysts are needed for both the nucleophilic addition to the carbonyl and the subsequent reduction step, especially when molecular hydrogen is involved. Reductive amination can be catalyzed by various transition metals,[19,20,21] even though precious metals such as Ru,[22–24] Pd[25,26] or Co[27,28] are the most commonly used. Despite its price, Rh also finds numerous applications for its remarkable activity and selectivity.[29–32]

Although the oil industry provides abundant carbonyl substrates, aiming to improve sustainability of amine production recent attention has shifted to bio-based substrates.[33–36] Furfural and benzaldehyde have been of particular interest in recent literature. In 2016, Chatterjee et al. reported the conversion of furfural to furfurylamine under mild conditions (80 °C, 20 bars of H_2 for 2 h) using aqueous ammonia.[37] With Rh/Al_2O_3 catalyst the reaction showed a remarkable selectivity (92%) and was applied to various substrates with good results. Aqueous ammonia was also used for the reductive amination of furfural in a recent study by Gao and co-workers, using a tailor-made Ru catalyst supported over a layered polymeric material which allowed a 99% yield in furfurylamine with only 2 equiv. of NH_3 per molecule of substrate.[38] An in-depth study of reductive amination of furfural on heterogeneous Ru- and Ni-based catalysts in aqueous ammonia was carried out by Gokhale and co-workers.[39] At 120–130 °C and 20 bar of H_2 for 10 h they succeeded in converting furfural directly from xylose or rice husk with yields ranging from 11 to 36%. Gomez and co-workers performed a detailed catalyst screening for the conversion of benzaldehyde to benzylamine in a methanolic ammonia solution, comparing Pt, Pd and Ru as active metal combined with different oxidative modifications for the active carbon as support.[40] It was found that Ru was the most active metal for catalysis and the modification with $(NH_4)_2S_2O_8$ improved the selectivity, and gave benzylamine in excellent yield (90 °C, 40 bars H_2) in less than 2 h. The study showed that the carbon-based support can be suitable and tuned for the reaction. In a recent study, Co nanoparticles encapsulated in graphene sheets were used for reductive amination of

[a] Dr. F. Bucciol, Prof. E. C. Gaudino, Prof. G. Cravotto, Prof. M. Manzoli
Department of Drug Science and Technology and NIS Interdepartmental Centre
University of Turin
Via Pietro Giuria 9
10125 Turin (Italy)
E-mail: emanuela.calcio@unito.it
maela.manzoli@unito.it
[b] Prof. A. Villa
Department of Chemistry
University of Milan
Via Golgi 19 – Corpo A
20133 Milan (Italy)
[c] Dr. M. C. Valsania
Department of Chemistry and NIS Interdepartmental Centre
University of Turin
Via Pietro Giuria 7
10125 Turin (Italy)

Supporting information for this article is available on the WWW under https://doi.org/10.1002/cplu.202300017

benzaldehyde to secondary amine using nitro-compounds as nitrogen source.[41] At 150 °C and 20 bars of H_2 for 6 h a wide range of substrates could be converted with excellent yield and selectivity, usually above 90%. The reaction rate can also be increased by using technologies such as microwaves (MW)[42] or ultrasound (US).[43] MW are electromagnetic waves ranging from 0.3 to 300 GHz, with most of the equipment working at 2.45 GHz. Unlike conventional heating, dielectric heating induces an oscillation of permanent and instantaneous dipoles in the irradiated material, which generates heat due to dielectric loss.[44–46] MW have been employed in chemical synthesis for their ability to reduce the reaction time, improve the energy efficiency and for the synergy with heterogeneous metal-based catalysts via the creation of localized hotspots.[47,48] Only few works exist on the application of MW for the reductive amination of aldehydes and ketones.[49] Recent examples include the synthesis of quinolines between amino-ketones and cyclic ketones,[50] where the MW decreased the reaction time to just 5 min at 160 °C but working in homogeneous conditions, and the reductive amination of both aldehydes and ketones using a heterogeneous bimetallic Pd/Cu catalyst embedded in a βCD framework using both H_2 and formic acid as hydrogen sources with yields up to 87% in just 2 h.[51] US are sound waves of frequency above 18 kHz, while most of their application in chemistry fall between 20–150 kHz. When US propagate through a liquid they induce cavitation: the formation and rapid collapse of vapor bubbles that can enhance the mass transfer and induce chemical reaction via high-energy microenvironments.[52,53] In this work we aim to (i) investigate the synergy between MW and various Rh-based heterogeneous catalysts for the reductive amination of aldehydes and ketones and (ii) highlight the effect of US in the preparation of homemade with highly dispersed and stable Rh. In this framework, two different carbon supports were used: commercial activated carbon and carbon nanofibers. The catalytic performances were compared to those obtained with commercial supported Rh catalysts. In the search of milder reaction conditions, as well as a more sustainable synthesis, we selected different bio-derived molecules as substrates for the reaction and aqueous ammonia as a cheap and nontoxic reagent. Ketones were chosen for the synthesis because few papers in the literature report their conversion.[54,55]

Results and Discussion

Reductive amination of aldehydes

A first screening of reaction conditions (Table 1) for the reductive amination of benzaldehyde over the commercial Rh/Al_2O_3 catalyst revealed that temperature and ammonia concentration play a crucial role over the selectivity: albeit conversion was always complete, below 80 °C only di-benzylamine was found (Table 1 entry 1). This is due to over-alkylation as side reaction: as benzylamine forms, it acts as a stronger nucleophile than NH_3 and thus reacts again with benzaldehyde. The concentration of NH_3 also plays an important role, since using 32 wt.% ammonia allowed an improvement of selectivity from 38.5% to 78.9% (Table 1 entry 3). However, it was not possible to further improve the results in the presence of commercial Rh/Al_2O_3. On this catalyst, despite some regions where Rh nanoparticle agglomerates have been observed by HR-TEM (Figure Supporting Information-**1**a, the Rh dispersion is very high (average diameter $d_m = 1.1 \pm 0.5$ nm, Figure Supporting Information-**1**b). According to the particle size distribution reported in Figure Supporting Information-**1**c, about 95% of the counted nanoparticles has size between 1 and 2 nm), resulting in a Rh SSA of 126.4 m^2/g. With this in mind, the use of commercial Rh/C (Table 2) surprisingly allowed the halving of reaction time and H_2 pressure with excellent results and even using 25 wt.% ammonia the yield was of 88.0% (Table 2 entry 4).

The two commercial catalysts have the same Rh loading (5 wt.%) and the results of the PXRD characterization summar-

Table 1. MW-assisted reductive amination of benzaldehyde over commercial Rh/Al_2O_3.

Entry	Ammonia [wt.%]	Time [h]	Temperature [°C]	H_2 [bar]	Conversion [%]	Sel. benzylamine [%]	Sel. di-benzylamine [%]	Yield [%]
1	25	2	50	20	100	0.0	100	0.0
2	25	2	80	20	100	38.5	61.5	38.5
3	32	2	80	20	100	78.9	21.1	78.9
4	32	2	80	10	100	58.9	41.1	58.9
5	32	1	80	20	100	34.7	65.3	34.7

Table 2. Comparison between Rh/Al_2O_3 and Rh/C commercial catalysts for benzaldehyde conversion under MW irradiation.

Entry	Catalyst	Ammonia [wt.%]	Time [h]	H_2 [bar]	Conversion [%]	Sel. benzylamine [%]	Sel. di-benzylamine [%]	Yield [%]
1	Rh/Al_2O_3	32	2	20	100	78.9	21.1	78.9
2	Rh/C	32	1	20	100	100	0.0	>99
3	Rh/C	32	1	10	100	98.2	1.8	98.2
4	Rh/C	25	1	10	100	88.0	12.0	88.0
5[a]	Rh/C	32	1	10	100	58.1	26.9	58.1

[a] Reaction performed under conventional heating (using Parr® device) without MW irradiation.

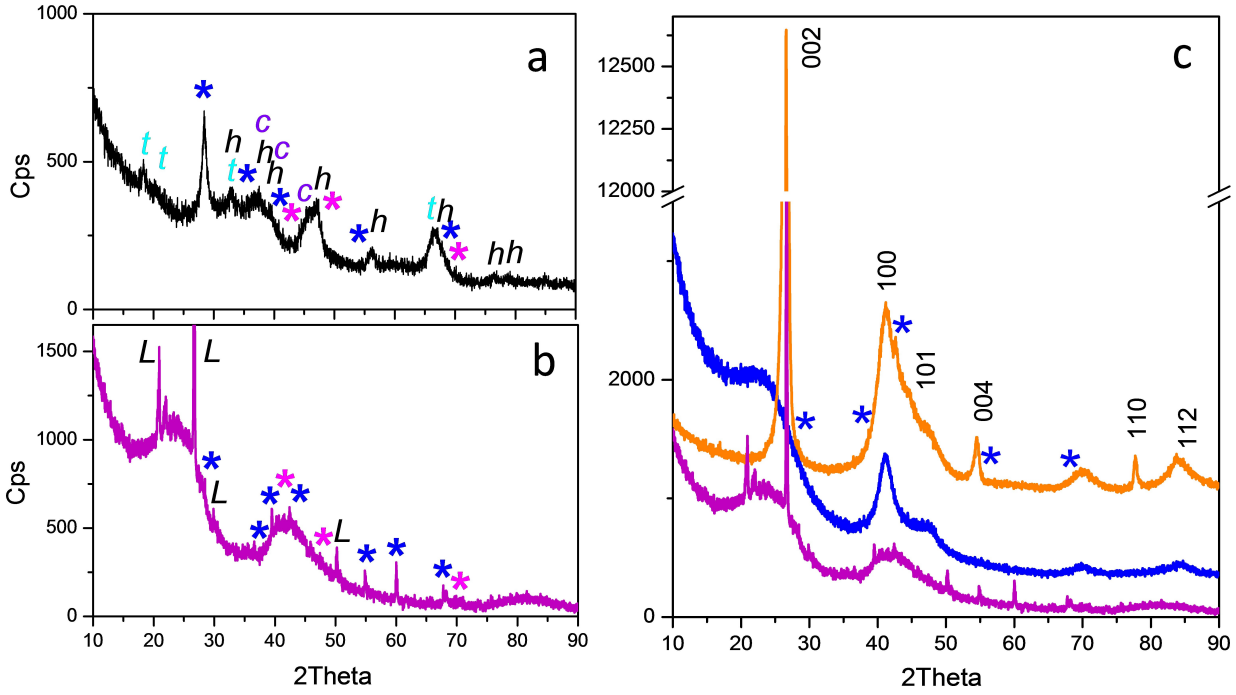

Figure 1. PXRD patterns of (a) Rh/Al_2O_3, (b) Rh/C commercial catalysts and (c) comparison among the PXRD patterns of commercial Rh/C (violet line), Rh/C US (blue line) and Rh/HHT US (orange line). Legend: t = tetragonal Al_2O_3 (file number 00-046-1131), h = hexagonal Al_2O_3 (file number 00-002-0921), c = cubic Al_2O_3 (file number 00-001-1303), blue * = tetragonal RhO_2 (file number 00-021-1315), pink * = cubic Rh (file number 00-001-1214), L = lignite-like phase (file number 00-005-0625), the Miller indexes of hexagonal graphite are reported in (c, file number 00-001-0646).

ized in Figure 1 reveal that the Rh crystalline phase is mainly in the form of tetragonal RhO_2 on both catalysts (signaled by blue asterisks), due to oxidation of the small Rh nanoparticles by air. In addition, very weak peaks related to metallic Rh (pink asterisks) have also been observed. In our reaction conditions activated carbon performed much better than alumina as a support, despite the same metal amount and that the opposite was claimed in literature.[37] An explanation of the observed behavior can be found in the different interaction between the supports and MW since with respect to alumina carbon is a better MW absorber.[56,57]

To confirm the role of MW in promoting the selectivity of reductive amination on heterogeneous Rh catalyst, the optimized MW-assisted benzylamine synthesis (Table 2, entry 3) was reproduced under conventional heating using a PARR® reactor (Table 2, entry 5). Although conventional heating provided complete benzaldehyde conversion in 1 h at 80 °C (10 bar of H_2), only half of the selectivity to benzylamine (58%) was recorded if compared to MW-assisted approach (98%) highlighting the crucial role of dielectric heating.

Even though benzaldehyde is not soluble in water, its suspension via vigorous stirring was sufficient to achieve good conversions. Nevertheless, we decided to dilute the aqueous ammonia in different solvents to improve its miscibility with the reaction media. For this purpose, a number of non-toxic and water-miscible solvents were selected: ethanol (EtOH), i-propanol (iPrOH), 1,2-pentanediol (1,2-PDO) and 1,3-pentanediol (1,3-PDO) (Figure 2).

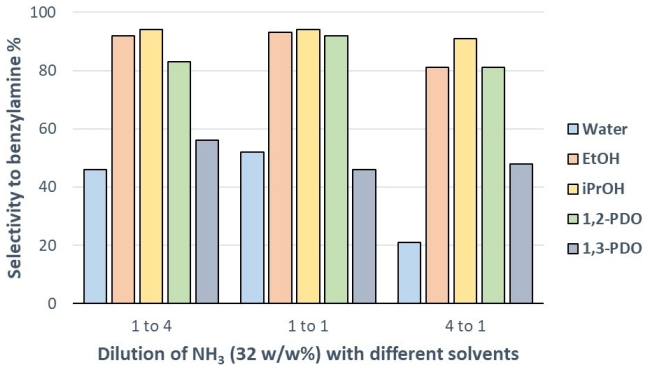

Figure 2. Solvent screening for benzaldehyde reductive amination. Different dilutions with ammonia: water (light blue), EtOH (orange), iPrOH (yellow), 1,2-PDO (green) and 1,3-PDO (Blue).

Different dilutions were also tested to find the best compromise between substrate solubilization and ammonia dilution. Conversion was always complete, however selectivity changed drastically depending on the solvent.

Firstly, all solvents performed better than a simple dilution in water showing that the solubilization of benzaldehyde in an organic solvent can indeed affect the result. The best selectivity (in the 92.1–94.0% range) towards benzylamine was found with the 1:1 solutions in EtOH, iPrOH or 1,2-PDO. These results show that NH_3 concentration can be decreased, as long as its viability to the substrate is maintained with the right solvent. We decided to run further tests using EtOH in a 1:1 dilution, since

Table 3. Reactions over substituted benzaldehyde and acetophenone derivatives in the presence of the commercial Rh/C catalyst.

Entry	Substrate	Solvent	Time [h]	H_2 [bar]	Conversion [%]	Selectivity [%]	Yield [%]
1	benzaldehyde	NH_3-EtOH 1:1	2	10	100	93.0	93.0
2	o-chlorobenzaldehyde	NH_3-EtOH 1:1	2	10	100	>99	>99
3	o-methoxy benzaldehyde	NH_3-EtOH 1:1	2	10	100	68.3	68.3
4	acetophenone	NH_3-EtOH 1:1	2	5	100	43.3	43.3
5	o-chloroacetopnenone	25 wt.%	2	5	53.7	9.3	5.0
6	o-methoxyacetophenone	25 wt.%	2	5	38.2	85.7	32.7
7	o-methoxyacetophenone	25 wt.%	4	5	98.9	58.5	57.9

EtOH is easier to handle than iPrOH and easier to remove from the crude if needed.

The use of alcohols as co-solvents allowed a further study using o-chlorobenzaldehyde and o-methoxy benzaldehyde, which would not have been possible using water (Table 3 entries 2 and 3). The results show that the chlorine substituent inhibits the over-alkylation completely, allowing a 100% yield of the primary amine.

This can be a useful tool since the chlorine is relatively easy to remove in reducing conditions. The methoxy substituent gave the opposite effect, lowering the selectivity towards the desired product. In the case of the acetophenone derivatives, the reduction to alcohol and the formation of the aliphatic amine were observed and, as for ρ-chloroacetophenone, the cleavage of the chlorine to produce acetophenone was the main side-reaction (Table Supporting Information-**1**).

A comparison between the commercial Rh/C catalyst and our homemade catalysts was performed with benzaldehyde as a substrate (Figure 3). The Rh/HHT PVA colloidal catalyst was completely inactive (data not shown): in this case the preparation method assured high Rh dispersion with $d_m = 1.3 \pm 0.2$ nm and Rh SSA equal to 166.9 m^2/g (Figure Supporting Information-**2**), but PVA likely shielded the Rh active sites under our reaction conditions. Conversion was complete in all the other experiments; however, as reported in Figure 3, the commercial Rh/C catalyst displayed the highest selectivity for benzylamine. Conversely, homemade Rh/C prepared under US (Rh/C US) showed activity for the reductive amination, but only yielded di-benzylamine. In this case, the PXRD characterization revealed no peaks related to crystalline Rh phases (Figure 1c, blue line). However, FESEM images acquired by both SE and BSE modes

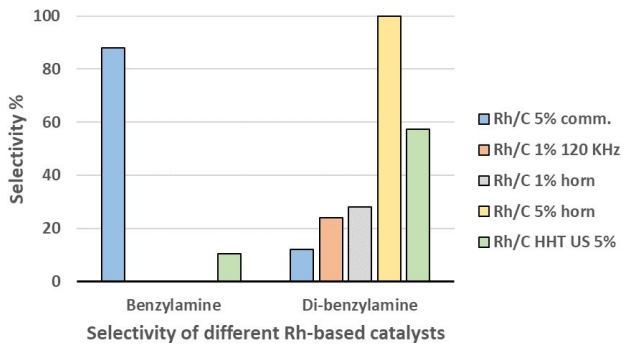

Figure 3. Selectivity of commercial and homemade catalysts for the reductive amination of benzaldehyde.

put in evidence the presence of Rh particles as bright spots, as confirmed by EDS analysis. In addition, Rh seems to decorate the borders of the particles of the support, which have globular morphology (Figure Supporting Information-**3**). Rh species appeared heterogeneous in size 5–15 nm, up to >100 nm Figure Supporting Information-**4**), but the presence of Rh was detected by EDS also in regions in which apparently no metal nanoparticles were present, as shown in Figure 4a), which indicates very high metal dispersion.

Interestingly, the HR-TEM measurements revealed the presence of Rh nanoparticle agglomerates (Figure 4b), nevertheless Rh is highly dispersed (Figure 4c, d) in agreement with the FESEM findings. The particle size distribution reported in Figure 4c is quite narrow, being the majority of the nanoparticles with size ranging between 2 and 4 nm, with a $d_m = 2.9 \pm 0.6$ nm and a Rh SSA of 74.7 m^2/g.

These results show that (i) US are beneficial for the activity of the prepared catalysts since they allowed to obtain highly dispersed Rh nanoparticles uniform in size and shape, (ii) the dispersion of Rh nanoparticles plays a key role in the conversion given the same metal loading, and also that (iii) carbon nanofibers are superior to activated carbon as support. However other factors, that deserve future investigations, seem to rule the selectivity, i.e. the presence of crystalline Rh and RhO_2 phases as well as the nature of the support, i.e. Al_2O_3 vs. carbon and type of carbon itself.

According to the PXRD results reported in Figure 1, with respect to the Norit graphitic carbon employed to prepare the catalyst by using US, the support of commercial Rh/C displays sharp and intense peaks and likely derived from vegetable sources. On the contrary, HHT CNTs expose defined graphitic planes.

Finally, the spacing measured in the Fast Fourier Transform of the HR-TEM image (2.20 Å, Figure 4d) is related to the (111) plane of metallic Rh nanoparticles in the crystalline cubic phase (00-001-1214). The small size of the Rh nanoparticles can explain why no peak due to the presence of crystalline metal phases was detected in the PXRD pattern.

FESEM analyses revealed that the Rh/C commercial catalyst shows similar features as for the metallic phase morphology and dispersion, i.e. the presence of Rh agglomerates with size ranging between 20 and 150 nm (Figure Supporting Information-**5**). However, with respect to the Rh/C US catalyst with the same metal loading, a lower abundance of Rh agglomerates homogeneously dispersed within the carbon matrix was observed in this case. Moreover, EDS mapping demonstrated

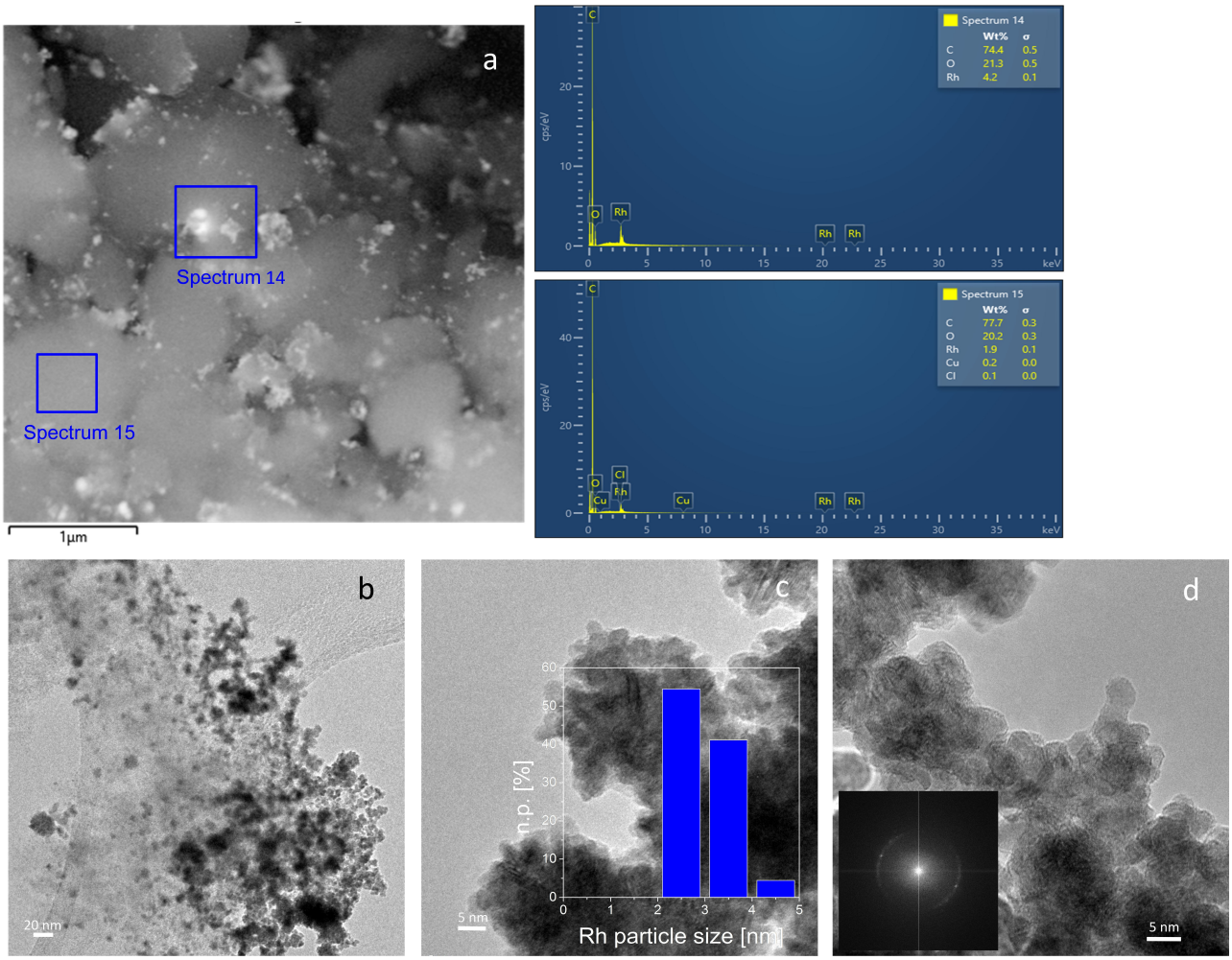

Figure 4. FESEM image of the Rh/C US catalyst acquired in SE mode in which the Rh particles appear brighter with respect to the support (a). Instrumental magnification 121000×. TEM representative images of Rh/C US (b,c), Rh particle size distribution, HR-TEM representative image with the corresponding Fast Fourier Transform (d). n.p. [%] represents the number of counted particles of diameter d_i. Instrumental magnification 50000×, 300000× and 400000×.

homogeneously highly dispersed Rh within the support (also in those regions of the sample where Rh was not clearly detected, see Figure 5a and b). Such feature indicates that the observed highly dispersed Rh species (Figure 5c, signaled by violet arrows) are produced along with crystalline Rh-containing phases during the synthesis of the commercial catalyst. Indeed, the particle size distribution built on FESEM images revealed that the Rh nanoparticles have an average diameter $d_m = 2.7 \pm 0.8$ nm, which results in a Rh SSA equal to 68.8 m^2/g.

Interestingly, Rh/HHT US not only converted all the benzaldehyde, but also yielded benzylamine, albeit in limited quantity (10.6%). On this catalyst, PXRD characterization revealed the presence of very weak peaks partially overlapped by the peaks of the support and due to tetragonal RhO_2 (blue asterisks in Figure 1b, orange curve). Indeed, due to the thermal treatment at high temperature to which the commercial HHT CNFs were submitted, the peaks related to hexagonal graphite were detected. Moreover, very small Rh nanoparticles with $d_m = 3.2 \pm 1.0$ nm and SSA = 62.9 m^2/g were observed by FESEM (Figure 5e).

Then, we moved to different substrates for the reaction (Figure 6). The experiments were performed in the presence of the commercial Rh/C catalyst. Benzaldehyde gave the best yields overall, followed by furfural. The two substrates were also less dependent on the solvent of choice. 3-phenylpropanal was instead highly influenced, since it gave no conversion in 25 wt.% aqueous ammonia, while the 1:1 dilution in EtOH allowed an 83.1% yield in 3-phenylpropylamine.

These results show that the reaction can be applied to different substrates, as long as the appropriate liquid medium is chosen. HMF was the only substrate to give the best yield (55.4%) in 25 wt.% ammonia: a higher concentration only resulted in over-alkylation while the dilution in EtOH was not beneficial.

Reductive amination of ketones

The optimization of reaction conditions for the reductive amination of acetophenone to phenylethylamine was per-

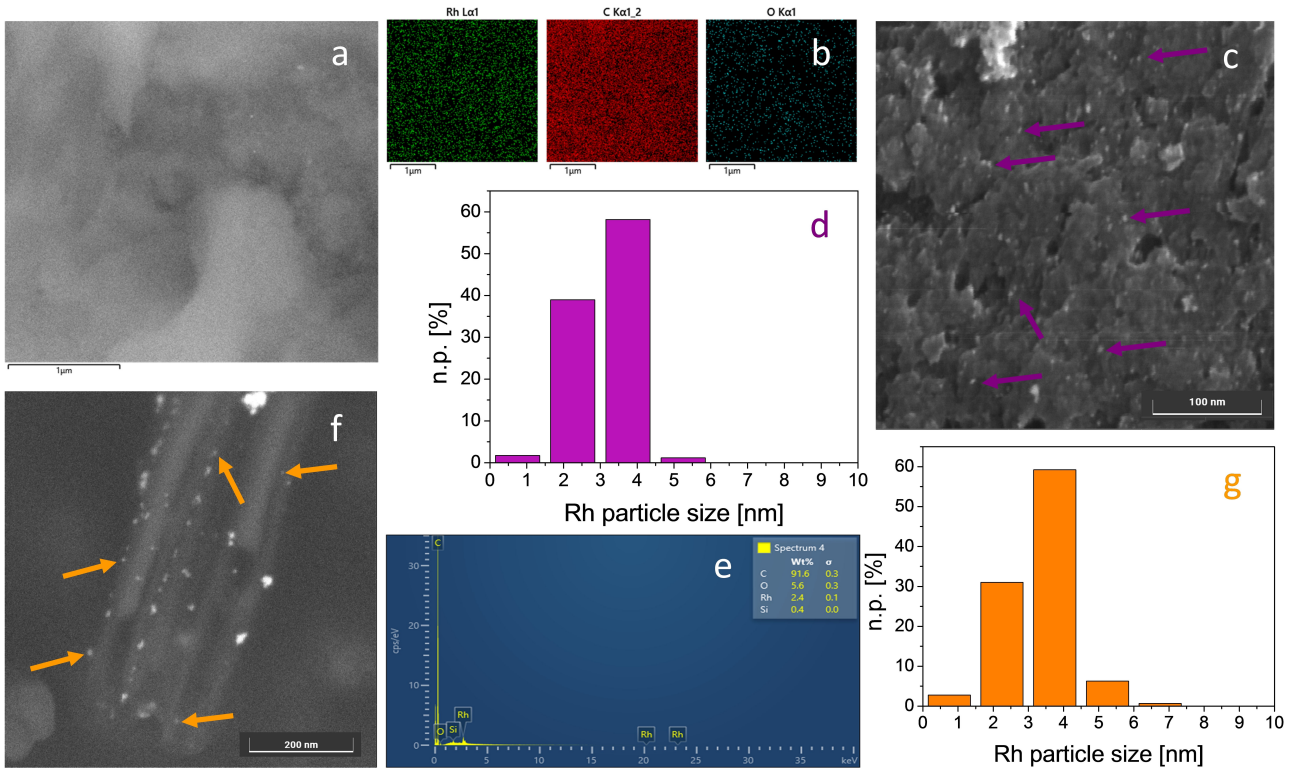

Figure 5. FESEM images of the Ru/C commercial catalyst (a,c), EDS maps of the region shown in a) for Rh, C and O (b) Rh particle size distribution (d) and EDS spectrum of the region shown in b) (e) and FESEM image of the Rh/HHT US catalyst (f) with the corresponding Rh particle size distribution (g). Images collected at 25 kV with the standard SE detector (a), at 5 kV with the SE detector in UH-resolution mode (c) and at 5 kV with the BSE detector in UH-resolution mode (f), n.p. [%] represents the number of counted particles of diameter d_i. Instrumental magnification: 240000× (a), 773000× (c) and 400000× (e).

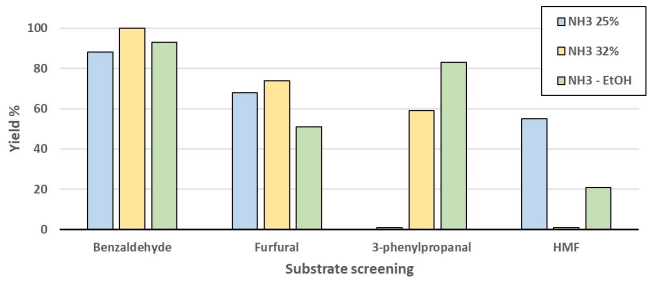

Figure 6. Yields achieved in the substrate screening over the commercial Rh/C catalyst with different ammonia concentrations. Reaction conditions: 80 °C, 10 bars of H_2, 2 h. Ammonia solution 25 wt.% (pale blue), 32 wt.% (pale orange) and NH_3-EtOH 1:1 (green).

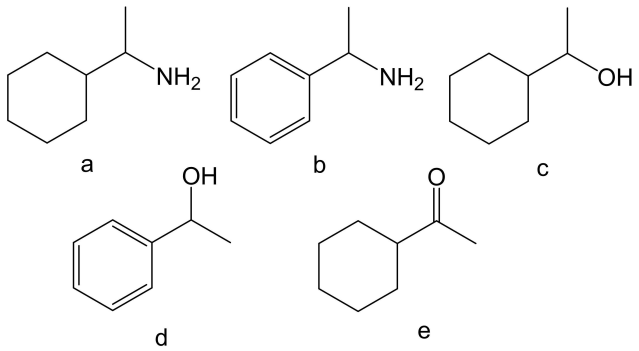

Scheme 1. Observed products of acetophenone MW-assisted reductive amination.

formed directly over the commercial Rh/C catalyst (Table 4), starting from the conditions found in literature for aldehydes: 80 °C, 20 bars of H_2, 2 h. Also, different concentrations of ammonia and the 1:1 dilution in EtOH were tested as well.

The conversion of acetophenone is good, if not complete, in all conditions. The selectivity towards the desired phenylethylamine (**d**) is however hampered by two side-reactions: the reduction of the carbonyl leading to phenyl ethanol (**b**) and the reduction of the aromatic ring, which can lead to several aliphatic compounds (Scheme 1). Thus, with respect to aldehydes, a lower hydrogen increasing pressure was needed, and the best yield (43.3%) was found under only 5 bars of H_2.

Further lowering the pressure to 3 bars improved the selectivity, but lowered the conversion, whereas the reaction time from 2 to 3 h in the same conditions improved the conversion from 65.9% to 98.1%, however it reduced the selectivity again, favoring the formation of (**b**) instead. The use of ϱ-chloroacetophenone and ϱ-methoxy acetophenone gave opposite results respect to benzaldehyde (Table 3 entries from 5 to 7), since the methoxy substituent strongly enhanced the selectivity (85.7%) towards the primary amine, impeding the reduction of the carbonyl group to alcohol. This, however, came at the price of a lower conversion (38.2%); increasing the reaction time to 4 h improved the conversion to 98.9%, leading

Table 4. Reaction conditions and catalyst screening for the MW-assisted reductive amination of acetophenone.

Entry	Catalyst	Time [h]	H_2 [bar]	Conversion [%]	Sel. a [%]	Sel. b [%]	Sel. c [%]	Sel. d [%]	Sel. e [%]	Yield [%]
1[a]	Commercial Rh/C	2	10	100	34.9	5.5	4.5	55.1	0.0	5.5
2[b]	Commercial Rh/C	2	10	100	32.7	10.9	5.4	51.0	0.0	10.9
3[c]	Commercial Rh/C	2	10	100	33.2	7.6	5.5	52.0	0.0	7.6
4[d]	Commercial Rh/C	2	10	100	13.0	0.0	8.8	78.2	0.0	0.0
5[a]	Commercial Rh/C	2	5	100	12.4	34.2	1.3	49.8	2.8	34.2
6[b]	Commercial Rh/C	2	5	100	12.0	43.3	0.8	42.1	1.8	43.3
7[b]	Commercial Rh/C	2	3	65.9	1.9	53.2	4.7	40.2	0.0	35.1
8[b]	Commercial Rh/C	3	3	98.1	7.5	35.2	1.9	49.9	0.0	34.5
9[b]	Rh/C US	2	5	1.1	0.0	0.0	0.0	100	0.0	0.0
10[b]	Rh/HHT US	2	5	56.4	0.0	43.8	3.9	52.3	0.0	24.7
11[b]	Rh/HHT US	3	5	54.0	0.0	49.2	0.0	47.8	2.9	26.6

[a] Ammonia 32 wt.%. [b] Ammonia 25 wt.%. [c] Ammonia 12 wt.%. [d] EtOH/NH_3 1:1.

to a final 57.9% yield. The comparison between the commercial Rh/C catalyst and our homemade Rh/HHT US catalyst gave better results than the tests over benzaldehyde. Indeed, even though the commercial catalyst was still the best performing, it was thus far possible to obtain a 26.6% yield in (**d**) over our catalyst (Table 4 entry 11). Rh/HHT US exhibited even a comparable selectivity towards (**d**) but suffered from a lower conversion. It is worth of note that the HHT carbon nanofibers used as support have a specific surface area of 37 m^2/g, with internal diameter of nanofibers in the 20–60 nm range,[58] whilst the activated carbon (Sigma Aldrich) has specific surface area of 1200 m^2/g, average pore radius 5.5 nm, total pore volume 0.80 cm^3/g, micropore volume 0.19 cm^3/g.[59] Therefore, the Rh dispersion (rather than the textural properties of the catalysts) is ruling the observed catalytic activity. This further suggest that on the Rh/HHT US catalyst the Rh dispersion is comparable to that observed for commercial Rh/C, in agreement with the obtained Rh SSA (62.9 m^2/g vs 68.8 m^2/g).

Finally, raspberry ketone and 1-hexanone were used as substrates for the reaction (Figure 7). The activity of commercial Rh/C and Rh/HHT US for the new substrates was also compared. Interestingly, Rh/HHT US was active for all substrates, and for raspberry ketone the activity was comparable with the commercial catalyst, allowing a 63.0% yield. Cyclohexanone was well converted to its amine over Rh/C (89.6% yield) while over Rh/HHT US its conversion was only 48.5% and the prevalent product was di-cyclohexylamine from over-alkylation.

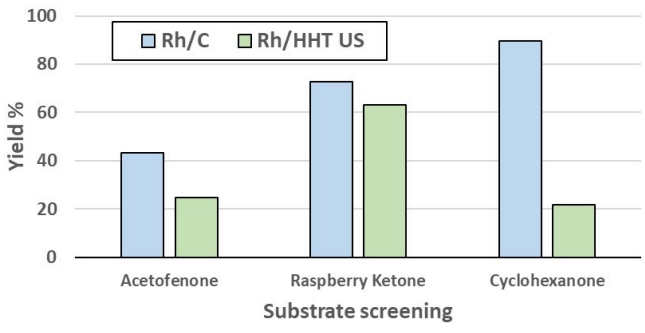

Figure 7. Substrate screening for the MW-assisted reductive amination of ketones over commercial Rh/C and Rh/HHT US.

The results show that the Rh/HHT US catalyst has a higher affinity for ketones than aldehydes.

On the stability of the catalysts under MW-assisted reductive amination conditions

The characterization results confirmed the important role of US in particle size dispersion of the Rh/HHT US catalyst. However, to demonstrate the superiority of the US home-made Rh catalyst with respect to the commercial Rh catalyst in the MW-assisted reductive amination of bio-derived molecules, the structure and morphology of the catalysts after MW-assisted reductive amination of benzaldehyde (reaction conditions: 80 °C, 10 bar H_2, 1 h) were investigated (Figure 8).

On one hand, the comparison of the PXRD patterns of the Rh/C commercial catalyst (Figure 8a) before (violet dashed line) and after reaction (wine line) put in evidence that the activated carbon support underwent to a strong structural modification, as demonstrated by the disappearance of the sharp peaks related to the lignite-like phase accompanied by new and less intense peaks at 2 Theta 18°, 41° and 47°. No peaks related to crystalline Rh phases were clearly observed. Indeed, the scaled-like surface morphology of the activated carbon support before reaction (Figure 5c) completely moved on a granular organization (Figure 8b, Figures Supporting Information-**6** and Supporting Information-**7**) in which the Rh particles (indicated by violet arrows in Figure 8b and showed in Figure Supporting Information-**8**) appear brighter with respect to the support.

In addition, the Rh particle size distribution (Figure 8c) revealed marked Rh agglomeration under MW-assisted reaction conditions, resulting in an increase of the nanoparticle dimensions, with $d_m = 34.6 \pm 14.7$ nm and a considerable drop of the Rh SSA to 5.1 m^2/g.

On the other hand, neither the structure and morphology of the HHT carbon nanofibers (Figures 8d-f) nor the Rh size (Figure 8e and **inset** of Figure 8f) underwent to significant changes upon MW-assisted reductive amination of benzaldehyde. In particular, the average diameter of the Rh nanoparticles increased to 3.3 ± 1.8 nm (from 3.2 ± 1.1 nm), with almost 70% of the nanoparticles with size ranging between 2

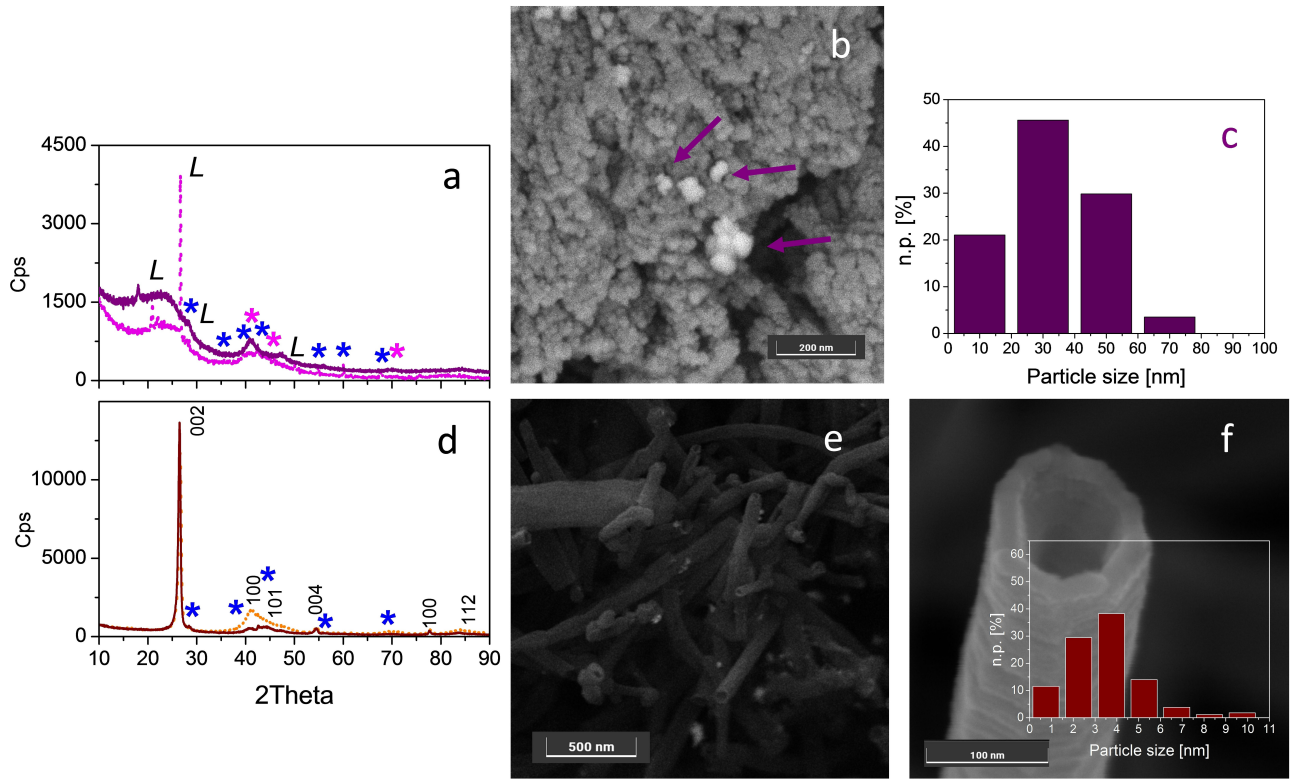

Figure 8. PXRD patterns of Rh/C commercial catalyst (a) and Rh/HHT US (b) after MW-assisted reductive amination of benzaldehyde (wine and brown lines, respectively. The patterns of the catalysts before reaction are reported for comparison (dashed lines). Legend: blue *=tetragonal RhO_2 (file number 00-021-1315), pink *=cubic Rh (file number 00-001-1214), *L*=lignite-like phase (file number 00-005-0625). FESEM images and Rh particle size distribution of Rh/C commercial catalyst (b and c, respectively) and Rh/HHT US (e,f and inset in f) after MW-assisted reductive amination of benzaldehyde. The images were acquired in BSE mode in which the Rh particles appear brighter with respect to the support (b,e) and In-beam SE mode (f). n.p. [%] represents the number of counted particles of diameter d_i. Instrumental magnification 300000×, 100000× and 912000×. Reaction conditions: 80 °C, 10 bar H_2, 1 h.

and 4 nm, which resulted in a decrease of the Rh SSA to 46.1 m^2/g (starting from 62.9 m^2/g). Interestingly, such decrease is much more contained than that occurred in the case of the Rh/C commercial catalyst. Therefore, the structural and morphological differences observed between the two recovered catalysts originated from the different stability under MW-assisted reaction conditions. Indeed, despite the lower conversion, the Rh/HHT US catalyst is much more stable than the commercial catalyst, likely due to the high temperature to which the carbon nanofibers that make up the support are submitted during preparation. As a matter of fact, the high temperature heating produced a support that is more resistant to the hotspots occurring during MW irradiation, thus also able to prevent Rh agglomeration. In both cases, EDS analyses revealed that the Rh amount is in agreement with the nominal metal loading.

Conclusion

A study on MW-assisted reductive amination of bio-derived aldehydes and ketones over heterogeneous Rh catalysts was presented. In search of milder reaction conditions, but also of a more sustainable and efficient process, the reactions were carried out under MW in order to shorten the reaction time, but also to improve the energy efficiency by synergy with heterogeneous Rh supported catalysts. Indeed, the use of MW combined with Rh catalysts allowed a mitigation of the reaction parameters, leading to a 98.2% yield in benzylamine (starting from benzaldehyde) working at 80 °C with 10 bar of H_2 for 1 h; and a 43.3% yield in phenylethylamine (from acetophenone) working at 80 °C with 5 bar of H_2 for 2 h. The rapid conversion and mild reaction conditions should broaden the potential applications. To the best of our knowledge, the only other relevant work for the reductive amination of acetophenone over a heterogeneous catalyst achieved a 44.0% yield working in significantly harsher H_2 pressure (80 bar) using both gaseous ammonia and ammonium chloride at 50 °C for 5 h reaction time.[60]

Aqueous ammonia solutions were employed as a cheap and abundant reactant, and in this framework, the use of different solvents improved the benzaldehyde solubility over the final yield and extended the substrate scope. Chlorine substituent improved the result over benzaldehyde allowing a complete yield in primary amine, whereas the methoxy substituent improved the selectivity for acetophenone, slowing down the formation of the correspondent alcohol. Screening of various substrates showed that the reaction could be readily converted; in particular, ketones were well converted over Rh/C, although

aldehydes are reported in the literature to be the preferred substrates for reductive amination.

Several homemade catalysts were synthetized and tested in both MW-assisted reductive amination reactions. US were proven to improve the activity of the catalysts compared to mechanical stirring, paving the way to the preparation of heterogeneous supported catalysts with lower metal loading. Moreover, carbon nanofibers proved to be a better support for the Rh nanoparticles than simple activated carbon, since Rh/HHT US proved to be much more stable than commercial Rh/C under MW-irradiation and despite a limited yield in benzylamine (10.6%), it allowed a high selectivity for the reductive amination of ketones and especially raspberry ketone, which was converted to raspberry amine with a 63.0% yield.

Experimental Section

Materials and methods

Benzaldehyde and its derivatives, acetophenone and its derivatives were all purchased from Merk. Cyclohexanone and 4-(4-hydroxyphenyl)-2-butanone were purchased from Merk. Furfural, hydroxymethyl furfural and 3-phenylpropionaldehyde were purchased from Alfa Aesar. HHT (High Heat Treated) carbon nanofibers (CNFs) were obtained from Applied Science Company (Cedarville, OH, USA). The activated carbon Norit CA1 from wood used in the deposition experiments was purchased from Merk. Rhodium(II) acetate ($(Rh(CO_2CH_3)_2)_2$) was purchased from Alfa Aesar (99.99%), sodium borohydride ($NaBH_4$, 99.99%) and poly(vinyl alcohol) (PVA, average molar weight 10,000, 87%–89% hydrolyzed) were used without any pre-treatment for the catalysts synthesis and they were purchased from Sigma-Aldrich (Haverhill, MA, USA). $RhCl_3$ was employed as metal precursor and purchased from Merk. Finally, commercial Rh/C, Rh 5 wt.% and Rh/Al_2O_3, Rh 5 wt.% catalysts were purchased from Merk.

Preparation of Rh-based catalysts. The colloidal Rh catalyst with 1 wt. % Rh was prepared according to a previously reported procedure.[61] The solution of $[Rh(CO_2CH_3)_2]_2$ was added to the capping agent PVA (Rh/PVA = 1/0.5 (wt/wt)) in 0.5 L of H_2O/EtOH = 1/1 vol/vol). Then, a fresh aqueous solution of $NaBH_4$ ($Rh/NaBH_4$ = 1/8 (mol/mol)) was added at once. The colloidal metal solution was supported on HHT CNFs (0.495 g) under vigorous stirring. By using sulphuric acid, the suspension was acidified to pH = 2 and stirred for 30 min in order to ensure the full immobilization of the nanoparticles on the support. The solid was filtered, washed with 0.5 L of H_2O and dried in oven at 80 °C for 1 day. This catalyst will be labelled as Rh/HHT PVA. For the other catalysts, the procedure used for the preparation was a wet impregnation. The amounts of support and Rh precursor were calculated to obtain a 5 wt.% Rh content. For the preparation of Rh/HHT CNFs 1 g of dry carbon nanofibers (HHT) was suspended in 50 mL of a hydroalcoholic (EtOH 50% vol/vol) 2 mg/mL solution of Rh/Cl_3.

Ultrasound (US) were applied through a horn transducer in contact with the liquid (21 kHz, 50 W) and were applied for three 10 min impulses, 5 min of silence was used in between to allow the temperature to drop. The beaker was placed inside an ice bath to reduce the increase in temperature. During the third ultrasound impulse, a stoichiometric quantity of $NaBH_4$ was added directly to the sample to reduce the nanoparticles. This catalyst will be labelled as Rh/HHT US. The preparation of Rh/C US followed the same procedure, only using Norit as support. The prepared catalysts were then filtered and washed two times with 50 mL of distilled water and one time with 50 mL of EtOH (50% vol/vol). The catalysts were finally dried at 80 °C overnight.

Characterization of Rh-based catalysts. Powder X-ray Diffraction (PXRD) patterns were collected with a PW3050/60 X'Pert PRO MPD diffractometer from PANalytical working in Bragg–Brentano geometry, using as a source the high-powered ceramic tube PW3373/10 LFF with a Cu anode (using Cu Kα1 radiation $\lambda = 1.5406$ Å) equipped with a Ni filter to attenuate Kβ. Scattered photons were collected by a real time multiple strip (RTMS) X'celerator detector. Data were collected in the $10° \leq 2\theta \leq 90°$ angular range, with 0.02° 2θ steps. The powdered samples were examined in their as-received form and posed in a spinning sample holder in order to minimize preferred orientations of crystallites.

The samples were characterized by high resolution transmission electron microscopy (HR-TEM) by using a 300 kV JEOL 3010-UHR instrument equipped with a LaB6 filament and with X-ray EDS analysis by a Link ISIS 200 detector. Digital micrographs were acquired by a (2k×2k)-pixel Ultrascan 1000 CCD camera and were processed by Gatan digital micrograph. Before the analyses, each sample in the form of powder was contacted with a lacey carbon Cu grid, which resulted in the adhesion of some particles to the sample holder by electrostatic interactions. Such procedure guaranteed to obtain a good dispersion of the sample particles and avoided any modification induced by the use of a solvent.

Field emission scanning electron microscopy (FESEM) measurements were carried out using a TESCAN S9000G FESEM 3010 microscope (30 kV), equipped with a high brightness Schottky emitter and Energy Dispersive X-ray Spectroscopy (EDS) analysis thanks to a Ultim Max Silicon Drift Detector (SDD, Oxford, Abingdon-on-Thames, UK). The samples were deposited on a stub that was coated with a conducting adhesive and inserted into the chamber in a fully motorized procedure. The samples were observed in their as-prepared forms without any metallization, whereas those after MW-assisted reductive amination of benzaldehyde (reaction conditions: 80 °C, 10 bar H_2, 1 h) were submitted to metallization with Cr (ca. 5 nm) to avoid any charging effect due to the possible presence of reaction products and intermediates (Emitech K575X sputter coater).

Histograms of the Rh particle size distribution (based on TEM or FESEM measurements) were obtained by considering a representative number of particles observed in the images for each sample and the mean particle diameter (d_m) was calculated by applying the following equation:

$$d_m = \Sigma d_i n_i / \Sigma n_i, \text{ being } n_i \text{ the number of particles with diameter } d_i.$$

Rh particles appeared well contrasted with respect to the supports and the counting was performed on electron micrographs obtained starting from 100000× magnification. Based on each particle size distribution, the corresponding Rh Specific Surface area (Rh SSA, m^2/g) of the supported metal nanoparticles was calculated by applying the formula (the nanoparticles are supposed to be spherical):

$$3\Sigma n_i r_i^2 / (\rho_{Rh} \Sigma n_i r_i^3)\ m^2/g$$

where r_i is the mean radius of the size class containing n_i particles, and ϱ_{Rh} the volumetric mass of Rh (12.42 g/cm^3). It is worth of note that direct comparisons were made between data coming from the characterisation by the same instrument.

Catalytic tests. Most of the reported catalytic experiments were performed inside a MW autoclave, SynthWAVE by Milestone srl. This is a multimode MW reactor equipped with multiple gas inlets, able to operate up to 300 °C and 199 bars. Temperature is controlled through a thermocouple and continuously adjusted. The MW cavity has a 1 L volume; however, the reactions were run in 15 mL glass vials immersed in 200 mL of brine solution. Mass transfer was provided through magnetic stirring. As a general procedure, 1 mmol of substrate were dissolved in 5 mL of the appropriate solvent and 10 mg of Rh catalyst (5 wt.%) were added. After the reaction the samples were filtered, and the products extracted in $CHCl_3$ for the GC-MS analysis.

For comparison, one catalytic test was performed with the optimized reaction conditions in a conventional PARR® pressure reactor 4842. The stainless-steel autoclave was filled with 25 mL of ammonia solution to which 50 mg of Rh/C (5 wt.%) and 5 mmol of substrate were added. Once closed, the reactor was flushed with N_2 and then filled with 10 bar of H_2.

GC-MS analysis. Samples were diluted in chloroform (ACS grade $\geq$99%) to a concentration of 2 mg/mL before the analysis. The GC-MS equipment used was an Agilent Technologies 6850 Network GC System fitted with a 5973 Network Mass Selective Detector, a 7683B Automatic Sampler and a capillary column Mega 5MS (length 30 m; i.d. 0.25 mm; film thickness 0.25 μm, Mega s.r.l., Legnano, Italy).

Reductive amination of aldehydes

The screening of solvent and reaction conditions for the reductive amination of aldehydes were firstly performed using benzaldehyde as substrate. The influence of time, temperature, hydrogen pressure and ammonia concentration was studied. The homemade catalysts were also compared to the commercial Rh/C. Finally, the optimal reaction conditions were applied for the conversion of furfural, hydroxymethyl furfural ad 3-phenylproprionaldehyde.

Optimization of reaction conditions. A screening and optimization of the reaction conditions was firstly performed using the commercial Rh/Al_2O_3 and Rh/C catalysts. We started from the conditions found in literature[37] (80 °C, 20 bars, 2 h) over the Rh/Al_2O_3 catalyst and progressively reduced the harshness of the parameters (Table 1). A NH_3 32 wt.% aqueous solution was initially used for the reaction, before testing more diluted aqueous and hydroalcoholic solutions. When the yield of benzylamine started to drop, we switched to the Rh/C catalyst and continued the process until the yield finally dropped below 90%. At that point the Rh/C and the homemade catalysts were compared.

Solvent screening. To investigate the effect of ammonia concentration over the reaction two aqueous solutions (32 wt.% and 25 wt.%) were used. Also, the 32 wt.% ammonia solution was diluted 1:4, 1:1 and 4:1 in various solvents: water, ethanol 96 v/v% (EtOH), isopropanol (*i*PrOH), 1,2-propandiol (1,2-PDO) and 1,3-propandiol (1,3-PDO). The screening of solvents was not only used to investigate the role of ammonia concentration, but also the impact of benzaldehyde solubility over the final yield.

Substrate screening. Using the optimized conditions for benzaldehyde, a screening of possible substrates was performed. At first, *p*-chlorobenzaldehyde and *o*-methoxybenzaldehyde were tested and compared to investigate the role of electron-withdrawing and electron-donating substituents over the reaction. Finally, we moved on to different aldehydes: albeit the reaction conditions were kept the same we tested three different ammonia solutions.

Reductive amination of ketones

Similarly, to what was done with benzaldehyde, we started using acetophenone as substrate. The reaction conditions were optimized and Rh/C and Rh/HHT US catalysts were compared. To conclude, a screening of different substrates was performed.

Optimization of reaction conditions. As for aldehydes, the catalytic experiments were performed at first at 80 °C with 20 bars of H_2 for 2 h. This time, the optimization was performed entirely with the commercial Rh/C catalyst. The reaction parameters were progressively reduced until the optimal conditions were found; at that point the commercial and homemade catalysts were compared in activity. To investigate the effect of ammonia concentration, 32 wt.% and 25 wt.% aqueous ammonia as well as 12 wt.% hydroalcoholic ammonia were used.

Substrate screening. Using the optimized conditions found for acetophenone, a substrate screening was performed. At first *o*-chloroacetophenone and *p*-methoxy acetophenone were tested to investigate the effect of electron-withdrawing and electron-donating groups over the reaction. Finally, raspberry ketone (4-(4-hydroxyphenyl)-2-butanone) and 1-hexanone were used as substrates.

Acknowledgements

E.C.G., G.C. and M.M. gratefully acknowledge the University of Turin for the financial support (Ricerca Locale 2022). Open Access funding provided by Università degli Studi di Torino within the CRUI-CARE Agreement.

Conflict of Interest

The authors declare no conflict of interest.

Data Availability Statement

The data that support the findings of this study are available in the supplementary material of this article.

Keywords: enabling technologies · heterogeneous catalysis · microwave chemistry · reductive amination · Rh nanoparticles · sonochemical synthesis

[1] A. Ricci, *Amino Group Chemistry: From Synthesis to the Life Sciences*, John Wiley & Sons, US, **2008**.
[2] S. A. Kelly, S. Pohle, S. Wharry, S. Mix, C. C. R. Allen, T. S. Moody, B. F. Gilmore, *Chem. Rev.* **2018**, *118*, 349–367.
[3] H. Lundberg, F. Tinnis, N. Selander, H. Adolfsson, *Chem. Soc. Rev.* **2014**, *43*, 2714–2742.
[4] B. Manteau, S. Pazenok, J. P. Vors, F. R. Leroux, *J. Fluorine Chem.* **2010**, *131*, 140–158.
[5] J. H. Ryu, P. B. Messersmith, H. Lee, *ACS Appl. Mater. Interfaces* **2018**, *10*, 7523–7540.
[6] S. Gong, S. Zhao, X. Chen, H. Liu, J. Deng, S. Li, X. Feng, Y. Li, X. Wu, K. Pan, *Macromol. Mater. Eng.* **2021**, *306*, 2100568.
[7] M. Janvier, L. Hollande, A. S. Jaufurally, M. Pernes, R. Ménard, M. Grimaldi, J. Beaugrand, P. Balaguer, P. H. Ducrot, F. Allais, *ChemSusChem* **2017**, *10*, 738–746.

[8] S. A. Lawrence, *Amines: synthesis, properties, and applications*, Cambridge University Press, Cambridge, **2004**.
[9] H. Setia Budi, Y. F. Mustafa, M. M. Al-Hamdani, A. Surendar, M. Ramezani, *Synth. Commun.* **2021**, *51*, 3694–3716.
[10] P. Colonna, S. Bezzenine, R. Gil, J. Hannedouche, *Adv. Synth. Catal.* **2020**, *362*, 1550–1563.
[11] A. R. Muci, S. L. Buchwald, in *Cross-coupling Reactions*, Springer, Berling, 1st edn., **2002**, 131–209.
[12] E. Podyacheva, O. I. Afanasyev, A. A. Tsygankov, M. Makarova, D. Chusov, *Synthesis* **2019**, *51*, 2667–2677.
[13] O. I. Afanasyev, E. Kuchuk, D. L. Usanov, D. Chusov, *Chem. Rev.* **2019**, *119*, 11857–11911.
[14] Q. Zou, F. Liu, T. Zhao, X. Hu, *Chem. Commun.* **2021**, *57*, 8588–8591.
[15] V. I. Tararov, R. Kadyrov, T. H. Riermeier, C. Fischer, A. Börner, *Adv. Synth. Catal.* **2004**, *346*, 561–565.
[16] J. S. Pan, R. Zhang, S. S. Ma, L. J. Han, B. H. Xu, *ChemistrySelect* **2020**, *5*, 10933–10938.
[17] C. Dong, Y. Wu, H. Wang, J. Peng, Y. Li, C. Samart, M. Ding, *ACS Sustainable Chem. Eng.* **2021**, *9*, 7318–7327.
[18] N. Wang, J. Liu, L. Tang, X. Wei, C. Wang, X. Li, L. Ma, *ACS Appl. Mater. Interfaces* **2021**, *13*, 24966–24975.
[19] J. Liu, Y. Song, L. Ma, *Chem. Asian J.* **2021**, *16*, 2371–2391.
[20] T. Irrgang, R. Kempe, *Chem. Rev.* **2020**, *120*, 9583–9674.
[21] D. Sui, F. Mao, H. Fan, Z. Qi, J. Huang, *Chin. J. Chem.* **2017**, *35*, 1371–1377.
[22] Y. Shi, J. Wang, F. Yang, C. Wang, X. Zhang, P. Chiu, Q. Yin, *Chem. Commun.* **2022**, *58*, 513–516.
[23] X. Li, S. D. Le, S. Nishimura, *Catal. Lett.* **2022**, *152*, 2860–2868.
[24] R. Sun, S. S. Ma, Z. H. Zhang, Y. Q. Zhang, B. H. Xu, *Org. Biomol. Chem.* **2023**, https://doi.org/10.1039/D2OB02312 A.
[25] S. Mahato, P. Rawal, A. K. Devadkar, M. Joshi, A. Roy Choudhury, B. Biswas, P. Gupta, T. K. Panda, *Org. Biomol. Chem.* **2022**, *20*, 1103–1111.
[26] L. E. Arteaga-Pérez, R. Manrique, F. Castillo-Puchi, M. Ortega, C. Bertiola, A. Pérez, R. Jiménez, *Chem. Eng. J.* **2021**, *417*, 129236.
[27] K. Murugesan, V. G. Chandrashekhar, T. Senthamarai, R. V. Jagadeesh, M. Beller, *Nat. Protoc.* **2020**, *15*, 1313–1337.
[28] V. G. Chandrashekhar, K. Natte, A. M. Alenad, A. S. Alshammari, C. Kreyenschulte, R. V. Jagadeesh, *ChemCatChem* **2021**, *14*, e202101234.
[29] S. Kirschtowski, C. Kadar, A. Seidel-Morgenstern, C. Hamel, *Chemie-Ingenieur-Technik* **2020**, *92*, 582–588.
[30] J. Bianga, N. Kopplin, J. Hülsmann, D. Vogt, T. Seidensticker, *Adv. Synth. Catal.* **2020**, *362*, 4415–4424.
[31] C. Nogues, G. Argouarch, *ChemistrySelect* **2020**, *5*, 8319–8327.
[32] L. Huang, Z. Wang, L. Geng, R. Chen, W. Xing, Y. Wang, *RSC Adv.* **2015**, *5*, 56936–56941.
[33] T. A. Gokhale, A. B. Raut, S. K. Chawla, B. M. Bhanage, *React. Chem. Eng.* **2022**, *7*, 1005–1013.
[34] T. Senthamarai, K. Murugesan, J. Schneidewind, N. V. Kalevaru, W. Baumann, H. Neumann, P. C. J. Kamer, M. Beller, R. V. Jagadeesh, *Nat. Commun.* **2018**, *9*, 4023–4034.
[35] J. Niemeier, R. V. Engel, M. Rose, *Green Chem.* **2017**, *19*, 2839–2845.
[36] V. Froidevaux, C. Negrell, S. Caillol, J. P. Pascault, B. Boutevin, *Chem. Rev.* **2016**, *116*, 14181–14224.
[37] M. Chatterjee, T. Ishizaka, H. Kawanami, *Green Chem.* **2016**, *18*, 487–496.
[38] M. Gao, X. Jia, J. Ma, X. Fan, J. Gao, J. Xu, *Green Chem.* **2021**, *23*, 7115–7121.
[39] T. A. Gokhale, A. B. Raut, B. M. Bhanage, *J. Mol. Catal.* **2021**, *510*, 111667.
[40] S. Gomez, J. A. Peters, J. C. Van der Waal, W. Zhou, T. Maschmeyer, *Catal. Lett.* **2002**, *84*, 1–5.
[41] L. Liu, W. Li, R. Qi, Q. Zhu, J. Li, Y. Fang, X. Kong, *J. Mol. Catal.* **2021**, *505*, 111504.
[42] S. Radhika, M. Neetha, T. Aneeja, G. Anilkumar, *Curr. Org. Chem.* **2020**, *24*, 2235–2255.
[43] M. Woltersdorf, R. Kranich, H.-G. Schmalz, *Tetrahedron* **1997**, *53*, 7219–7230.
[44] G. Cravotto, D. Carnaroglio, *Microwave Chemistry*, De Gruyter, 1st edn., **2017**.
[45] K. K. Rana, S. Rana, *OALib* **2014**, *01*, 1–20.
[46] C. Gabriel, S. Gabriel, E. H. Grant, B. S. J. Halstead, D. Michael, P Mingos, *Chem. Soc. Rev.* **1998**, *27*, 213–223.
[47] K. Martina, G. Cravotto, R. S. Varma, *J. Org. Chem.* **2021**, *86(20)*, 13857–13872.
[48] Y. Tsukahara, A. Higashi, T. Yamauchi, T. Nakamura, M. Yasuda, A. Baba, Y. Wada, *J. Phys. Chem. C* **2010**, *114*, 8965–8970.
[49] M. Manzoli, E. Calcio Gaudino, G. Cravotto, S. Tabasso, R. B. N. Baig, E. Colacino, R. S. Varma, *ACS Sustainable Chem. Eng.* **2019**, *7(6)*, 5963–5974.
[50] H. V. Bailey, M. F. Mahon, N. Vicker, B. V. L. Potter, *ChemistryOpen* **2020**, *9*, 1113–1122.
[51] E. Calcio Gaudino, E. Acciardo, S. Tabasso, M. Manzoli, G. Cravotto, R. S. Varma, *Molecules* **2020**, *25*, 410.
[52] R. Martínez, G. Cravotto, P. Cintas *J. Org. Chem.* **2021**, *86(20)*, 13833–13856.
[53] Z. Wu, S. Tagliapietra, A. Giraudo, K. Martina, G. Cravotto, *Ultrason. Sonochem.* **2019**, *52*, 530–546.
[54] J. W. Park, Y. K. Chung, *ACS Catal.* **2015**, *5*, 4846–4850.
[55] Z. Luo, S. Wan, Y. Pan, Z. Yao, X. Zhang, B. Li, J. Li, L. Xu, Q.-H. Fan, *Asian J. Org. Chem.* **2022**, *11*, e202100707.
[56] A. L. Garcia-Costa, J. A. Zazo, J. J. Rodriguez, J. A. Casas, *Appl. Catal. B* **2017**, *218*, 637–642.
[57] L. Ge, X. Liu, H. Feng, H. Jiang, T. Zhou, H. Chu, Y. Zhang, C. Xu, Z. Wang, *Fuel* **2022**, *314*, 123140.
[58] I. Barlocco, S. Bellomi, J. J. Delgado, X. Chen, L. Prati, N. Dimitratos, A. Roldan, A. Villa, *Catal. Today* **2021**, *382*, 61–70.
[59] S. Capelli, D. Motta, C. Evangelisti, N. Dimitratos, L. Prati, C. Pirola, A. Villa, *Nanomaterials* **2020**, *10*, 505.
[60] T. Ikenaga, K. Matsushita, J. Shinozawa, S. Yada, Y. Takagi, *Tetrahedron* **2005**, *61*, 2105–2109.
[61] I. Barlocco, S. Capelli, E. Zanella, X. Chen, J. J. Delgado, A. Roldan, N. Dimitratos, A. Villa, *J. Energy Chem.* **2020**, *52*, 301–309.

Manuscript received: January 10, 2023
Revised manuscript received: March 8, 2023